Inorganic Chemistry

Article

pubs.acs.org/IC

Heterobimetallic μ-Oxido Complexes Containing Discrete $V^{V}-O-M^{III}$ (M = Mn, Fe) Cores: Targeted Synthesis, Structural Characterization, and Redox Studies

Kisholoy Bhattacharya,[†] Sk Md Towsif Abtab,[†] Mithun Chandra Majee,[†] Akira Endo,[‡] and Muktimoy Chaudhury*,[†]

[†]Department of Inorganic Chemistry, Indian Association for the Cultivation of Science (IACS), Jadavpur, Kolkata 700032, India

[‡]Department of Materials and Life Sciences, Faculty of Science and Technology, Sophia University, 7-1 Kioi-cho, Chiyoda-ku, Tokyo 102-8554, Japan

Supporting Information

ABSTRACT: Heterobimetallic compounds $[L'OV^{V}(\mu\text{-}O)\text{-}M^{III}L]_n$ (n = 1, M = Mn, **1**–**5**; n = 2, M = Fe, **6** and **7**) containing a discrete unsupported $V^{V}-O-M^{III}$ bridge have been synthesized through a targeted synthesis route. In the V–O–Mn-type complexes, the vanadium(V) centers have a square-pyramidal geometry, completed by a dithiocarbazate-based tridentate Schiff-base ligand (H_2L'), while the manganese(III) centers have either a square-pyramidal (**1** and **3**) or an octahedral (**2** and **5**) geometry, made up of a Salen-type tetradentate ligand (H_2L) as established by X-ray diffraction analysis. The V–O–Mn bridge angle in these compounds varies systematically from 155.3° to 128.1° in going from **1** to **5** while the corresponding dihedral angle between the basal planes around the metal centers changes from 86.82° to 20.92°, respectively. The V–O–Fe-type complexes (**6** and **7**) are tetranuclear, in which the two dinuclear V(μ-O)Fe units are connected together by apical iron(III)–aryl oxide interactions, forming a dimeric structure with a pair of Fe–O–Fe bridges. The X-ray data also confirm the V=O → M canonical form to contribute predominantly on the overall V–O–M bridge structure. The molecules in solution also retain their heterobinuclear composition, as established by electrospray ionization mass spectrometry and ^{51}V NMR spectroscopy. Electrochemically, these complexes are quite interesting; the manganese(III) complexes (**1**–**5**) display three successive reductions (processes I–III), each with a monoelectron stoichiometry. Process I is due to a Mn^{III}/Mn^{II} reduction ($E_{1/2}$ ranges between −0.32 and −0.05 V), process II is a ligand-based reduction, and process III ($E_{1/2}$ = ∼1.80 V) owes its origin to a $V^{V}O/V^{IV}O$ reduction; all potentials are versus Ag/AgCl. The iron(III) compounds (**6** and **7**), on the other hand, show at least four irreversible processes, appearing at E_{pc} = −0.20, −1.0, −1.58, and −1.68 V in compound **6** (processes IV–VII), together with a reversible process (process VIII) at $E_{1/2}$ = −1.80 V (ΔE_p = 80 mV). While the first two of these are due to Fe^{III}/Fe^{II} reductions at the two iron(III) centers of these tetranuclear cores, the reversible reduction at a more negative potential (ca. −1.80 V) is due to a $V^{V}O/V^{IV}O$-based electron transfer.

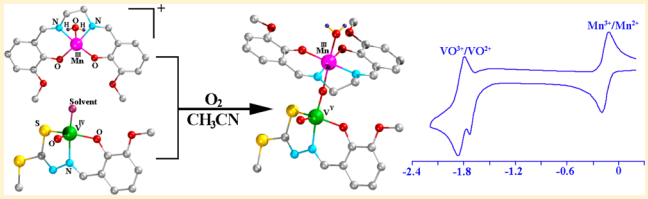

INTRODUCTION

The chemistry of heterobimetallic complexes containing the M–O–M′ framework is a topic of contemporary research interest.[1] Nature has often used heterobimetallic systems quite judiciously to catalyze many important reactions in biology. Superoxide dismutase and the CuB···cyt-a_3 component of cytochrome c oxidase are the classic examples of similar enzymes.[2] The properties of such dissimilar metal-ion assemblies often change significantly because of their cooperative influences. These observations have motivated coordination chemists to develop protocols for the syntheses of heterobimetallic compounds, connected by an unsupported oxido bridge, to be used as a catalyst for various fundamental reactions.[1a,3]

Vanadium in higher oxidation states (5+ and 4+) is oxophilic. It forms various types of oxido species depending on the charge and denticity of the coordinating ligand attached to the metal centers.[4] Among these compounds, those containing the $[V_2O_3]^{n+}$ (n = 2–4) cores belong to the largest family, reported thus far in which the isovalent (V^{IV}_2, V^{V}_2) or mixed-valent vanadium (V^{IV}–V^{V}) centers are connected by a V–O–V bridge.[5] About 40 such divanadium compounds have been crystallographically characterized to date in which both of the vanadium centers have identical coordination environments.[5] Contrary to this, only a few heterobimetallic compounds containing a V–O–M core have been as yet crystallographically characterized.[6]

For quite sometime, we have had an ongoing project for the syntheses of divanadium compounds containing V_2O_3 core.[7−10] In a sequel to that, lately we have developed a protocol for the targeted synthesis of hither-to-unknown μ-oxidodivanadium(V) compounds with coordination asymmetry that contain octahedral and square-pyramidal vanadium(V) centers.[9,10] To achieve

Received: March 12, 2014
Published: August 1, 2014

   dx.doi.org/10.1021/ic501563r | Inorg. Chem. 2014, 53, 8287–8297

that goal, we opted for tetradentate Schiff-base ligand *N*,*N*′-bis(salicylidene)-1,2-diaminoethane (H_2Salen) to generate the octahedral vanadium sites, while for the square-pyramidal centers, tridentate biprotic dithiocarbazate-based ligands (H_2L') have been used, as detailed elsewhere.[9,10] In a recent communication,[11] we recast that methodology to our advantage to make it useful for the targeted syntheses of heterobimetallic μ-oxido compounds containing a discrete V^V-O-Fe^{III} core. Herein, we made an effort to use the same modified methodology for the preparation of compounds containing a discrete V^V-O-Mn^{III} core (**1**−**5**) in order to test the efficacy of this protocol as a general method for the synthesis of compounds containing a V−O−M core. New families of (i) binuclear $[L'OV^V(\mu\text{-}O)Mn^{III}L]$ [$L' = L^2$, $L = L^4$, **1**; L^3, L^5, **2**; L^1, L^6, **3**; L^1, L^7, **4**; L^2, L^8, **5**] and (ii) tetranuclear $[L'OV^V(\mu\text{-}O)Fe^{III}L]_2$ [L^1, L^5, **6**; L^2, L^5, **7**] compounds have been synthesized. Their characterizations by single-crystal X-ray diffraction analysis, ^{51}V NMR spectroscopy, and electrospray ionization mass spectrometry (ESI-MS) studies are reported. The redox properties of the compounds have been investigated in detail.

EXPERIMENTAL SECTION

Materials. The solvents were reagent grade, dried by standard procedure,[12] and distilled under nitrogen prior to their use. The tridentate dithiocarbazate-based ligands *S*-methyl-3-(2-hydroxyphenyl)-methylenedithiocarbazate (H_2L^1), *S*-methyl-3-(5-bromo-2-hydroxyphenyl)methylenedithiocarbazate (H_2L^2), and *S*-methyl-3-(3-methoxy-2-hydroxyphenyl)methylenedithiocarbazate (H_2L^3) and the tetradentate Salen-based Schiff-base ligands *N*,*N*′-bis(2-benzoyl-1-methylethylidene)-1,2-diaminoethane (H_2L^4), *N*,*N*′-bis(3-methoxysalicylidene)-1,2-diaminoethane (H_2L^5), *N*,*N*′-bis(5-chlorosalicylidene)-2,3-dimethyl-2,3-diaminobutane (H_2L^6), *N*,*N*′-bis(5-bromosalicylidene)-2,3-dimethyl-2,3-diaminobutane (H_2L^7), and *N*,*N*′-bis(3-methoxysalicylidene)-2,3-dimethyl-2,3-diaminobutane (H_2L^8) were prepared following the reported procedure.[13,14] $[MnL^4Cl]$,[15] $[MnL^5(H_2O)]ClO_4$,[16a] $[FeL^5Cl]_2$,[16b] and $Mn(OAc)_3{\cdot}2H_2O$[17] were prepared following reported methods. All other reagents were commercially available and used as received.

Preparation of the Complexes. *$[L^2OV^V(\mu\text{-}O)Mn^{III}L^4]$ (**1**).* To a stirred acetonitrile (25 mL) solution of $[L^4MnCl]$[15] (110 mg, 0.25 mmol) was added solid $AgNO_3$ (40 mg, 0.25 mmol). The stirring was continued for 0.5 h. Precipitated AgCl was filtered through a Celite bed. In another reaction pot, solid H_2L^2 (75 mg, 0.25 mmol) was added to a solution of $[VO(acac)_2]$ (65 mg, 0.25 mmol) in acetonitrile (25 mL) and refluxed for 0.5 h to obtain a greenish-brown solution. The solution was combined with the previous filtrate, and the combined solution was refluxed further for 2 h and cooled to room temperature. It was then filtered. The filtrate volume was reduced to ca. 25 mL by rotary evaporation and kept in a refrigerator for an overnight period to get a dark-brown crystalline product. It was collected by filtration, washed with acetonitrile, and dried over $CaCl_2$. Yield: 70 mg (32%). Anal. Calcd for $C_{31}H_{29}N_4O_5S_2VMnBr$: C, 47.28; H, 3.71; N, 7.11; Mn, 6.98; V, 6.48. Found: C, 47.44; H, 3.59; N, 7.19; Mn, 7.12; V, 6.35. FT-IR bands (KBr pellets, cm^{-1}): 1597s, 1508vs, 1438s, 1456s, 1398s, 1292s, 958s, 858s, 696s. ESI-MS (positive) in CH_2Cl_2: m/z 810 ($[M + Na]^+$), 401 ($[MnL^4]^+$).

*$[L^3OV^V(\mu\text{-}O)Mn^{III}(H_2O)L^5]{\cdot}2CH_3CN$ (**2**).* To a solution of $[VO(acac)_2]$ (65 mg, 0.25 mmol) in acetonitrile (25 mL) was added solid H_2L^3 (65 mg, 0.25 mmol), and the combination was refluxed for 0.5 h to get a greenish-brown solution. It was then added to a stirred solution of $[L^5Mn(H_2O)]ClO_4$[16a] (113 mg, 0.25 mmol) in acetonitrile (20 mL) and kept in the open air for an overnight period to obtain a brown crystalline product. It was collected by filtration, washed with CH_3CN, and dried over $CaCl_2$. Yield: 62 mg (30%). Anal. Calcd for $C_{32}H_{36}N_6O_9S_2VMn$: C, 46.95; H, 4.43; N, 10.27; Mn, 6.72; V, 6.23. Found: C, 46.64; H, 4.49; N, 10.18; Mn, 6.68; V, 6.29. FT-IR bands (KBr pellets, cm^{-1}): 1625vs, 1600s, 1533m, 1545m, 1463s, 1440s, 1301s, 1251s, 1218s, 1081s, 1041m, 945s, 858vs, 731s, 653m. ESI-MS (positive) in CH_2Cl_2: m/z 741 ($[M - H_2O - 2CH_3CN + Na]^+$), 381 ($[MnL^5]^+$).

*$[L^1OV^V(\mu\text{-}O)Mn^{III}L^6]$ (**3**).* To a solution of $Mn(OAc)_3{\cdot}2H_2O$ (67 mg, 0.25 mmol) in acetonitrile (25 mL) was added the solid ligand H_2L^6, and the solution was refluxed for 1 h. After reflux, the solution was filtered, and the filtrate was taken in a conical flask. In another reaction pot, $[VO(acac)_2]$ (65 mg, 0.25 mmol) was added to a solution containing H_2L^1 (55 mg, 0.25 mmol) in acetonitrile (25 mL) and refluxed for 0.5 h. The solution was filtered, and the filtrate was added to the previous solution under stirring. The combined solution was kept in air for an overnight period to obtain a dark-brown crystalline product. The product was collected by filtration, washed with CH_3CN, and dried over $CaCl_2$. Yield: 66 mg (35%). Anal. Calcd for $C_{29}H_{28}N_4O_5S_2MnVCl_2$: C, 46.23; H, 3.75; N, 7.44, Mn, 7.30; V, 6.77. Found: C, 46.46; H, 3.50; N, 7.42; Mn, 7.38; V, 6.68. FT-IR bands (KBr pellets, cm^{-1}): 1604vs, 1545s, 1525s, 1452m, 1381m, 1301s, 1147s, 1018w, 962s, 852s, 785w, 682m, 657m, 534m. ESI-MS (positive) in CH_2Cl_2: m/z 446 ($[MnL^6]^+$).

*$[L^1OV^V(\mu\text{-}O)Mn^{III}L^7]$ (**4**).* This compound was prepared following essentially the same procedure as that described for compound **3** using H_2L^7 instead of H_2L^6. Yield: 39%. Anal. Calcd for $C_{29}H_{28}N_4O_5S_2MnVBr_2$: C, 41.35; H, 3.35; N, 6.65; Mn, 6.53; V, 6.05. Found: C, 41.17; H, 3.23; N, 6.71; Mn, 6.54; V, 6.02. FT-IR bands (KBr pellets, cm^{-1}) 1604vs, 1545m, 1525m, 1301s, 1147s, 962s, 852s, 758m, 682m, 657m, 534m. ESI-MS (positive) in CH_2Cl_2: m/z 535 ($[MnL^7]^+$).

*$[L^2OV^V(\mu\text{-}O)Mn^{III}(H_2O)L^8]{\cdot}CH_3CN$ (**5**).* This compound was prepared following the same procedure as that described for compound **3** using H_2L^8 instead of H_2L^6 and H_2L^2 instead of H_2L^1. Yield: 33%. Anal. Calcd for $C_{33}H_{38}N_5O_8S_2BrMnV$: C, 44.91; H, 4.34; N, 7.93; Mn, 6.23; V, 5.78. Found: C, 44.75; H, 4.27; N, 7.82; Mn, 6.50; V, 5.75. FT-IR bands (KBr pellets, cm^{-1}): 1601vs, 1542s, 1523s, 1450m, 1383s, 1300s, 1144s, 1015w, 964s, 853s, 783w, 681m, 657m, 533m. ESI-MS (positive) in CH_2Cl_2: m/z 437 ($[MnL^8]^+$).

*$[L^1OV^V(\mu\text{-}O)Fe^{III}L^5]_2{\cdot}CH_3CN$ (**6**).* To a stirred acetonitrile solution (25 mL) of $[L^5FeCl]_2$ (83 mg, 0.2 mmol) was added $AgNO_3$ (70 mg, 0.4 mmol), and the stirring was continued for 0.5 h more. The solution was filtered through a Celite bed to remove the precipitated AgCl, and the filtrate was taken into a conical flask. In a separate reaction pot, a stoichiometric amount (90 mg, 0.4 mmol) of the solid ligand H_2L^1 was added to a stirred solution of $[VO(acac)_2]$ (104 mg, 0.4 mmol) in acetonitrile (25 mL), and the resulting solution was refluxed for 0.5 h. Both solutions were combined, stirred for about 1 h, and kept overnight in air to obtain dark-brown crystals. The compound was isolated by filtration, washed with hexane, and finally dried in a desiccator over $CaCl_2$. Yield: 74 mg (42%). Anal. Calcd for $C_{56}H_{55}N_9O_{14}S_4V_2Fe_2$: C, 47.35; H, 3.87; N, 8.87; V, 7.19; Fe, 7.99. Found: C, 47.53; H, 3.87; N, 9.04; V, 7.11; Fe, 7.85. FT-IR bands (KBr pellets, cm^{-1}): 1626vs, 1599vs, 1444vs, 1250vs, 1222m, 968s, 841s, 735s. ESI-MS (positive) in CH_3CN: m/z 382 ($[L^5Fe]^+$).

*$[L^2OV^V(\mu\text{-}O)Fe^{III}L^5]_2{\cdot}CH_3CN$ (**7**).* This compound was obtained as a dark-brown crystalline product following essentially the same procedure as that for compound **6** using the ligand H_2L^2 instead of H_2L^1. Yield: 38.5%. Anal. Calcd for $C_{56}H_{53}N_9O_{14}S_4Br_2V_2Fe_2$: C, 42.63; H, 3.39; N, 7.99; V, 6.47; Fe, 7.06. Found: C, 42.43; H, 3.47; N, 8.12; V, 6.51; Fe, 6.98. FT-IR bands (KBr pellets, cm^{-1}): 1625vs, 1598vs, 1444s, 1249s, 1220m, 970s, 842s, 735s. ESI-MS (positive) in CH_3CN: m/z 382 ($[L^5Fe]^+$).

Physical Measurements. Elemental (C, H, and N) analyses were performed at IACS on a PerkinElmer model 2400 series II CHNS analyzer. IR, ESI-MS, and ^{51}V NMR spectra were recorded using the same instrumentation facilities as those described elsewhere.[18] Cyclic voltammetry (CV) scans of the compounds were recorded in *N*,*N*-dimethylformamide (DMF) because of solubility restrictions. The stabilities of the solutions were checked through electrical conductivity measurement using a Systronics (India) model 306 conductivity bridge. In all cases, solutions were virtually nonconducting for a couple of hours before showing a slow increase in the conductivity with time. A BAS model 100 B/W electrochemical workstation coupled with a glassy carbon working electrode and a platinum wire counter electrode was employed. Ag/AgCl was used for reference and a ferrocenium/ferrocene

dx.doi.org/10.1021/ic501563r | *Inorg. Chem.* 2014, 53, 8287−8297

Scheme 1. Schematic Presentation for the Formation of Compounds 1−5[a]

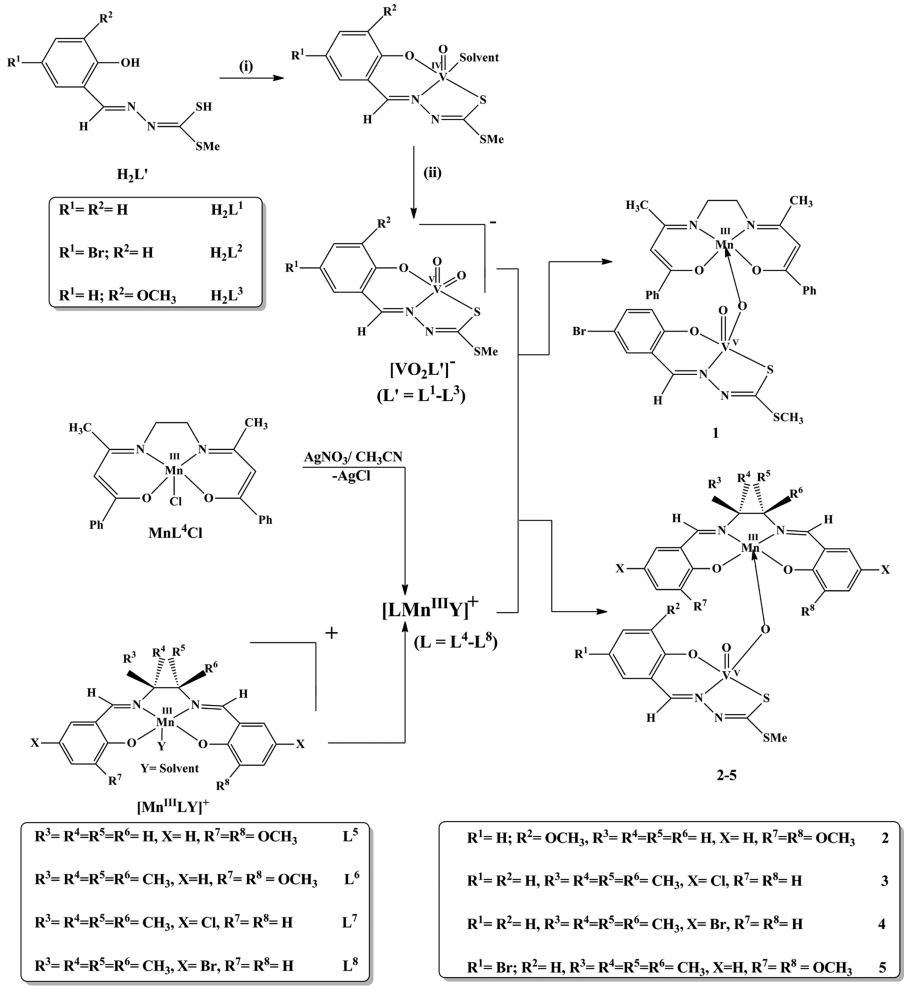

[a]Conditions: (i) $[VO(acac)_2]$ in acetonitrile; (ii) cation-assisted aerial oxidation. Compounds **2** and **5** contain an axially coordinated H_2O molecule to the manganese(III) center, not shown in the figure.

(Fc/Fc^+) couple as the internal standard.[19] Solutions were ∼1.0 mM in samples and contained 0.1 M tetrabutylammonium perchlorate (TBAP) as the supporting electrolyte.

Analysis of metal ions (V, Fe, and Mn) was carried out in triplicate by inductively coupled plasma optical emission spectrometry (ICP-OES) with a PerkinElmer model Optima 2000 DV instrument. A radio-frequency power of 1300 W under an argon gas flow (Nebulizer, 0.86 L/min; Auxillary, 1.2 L/min; Plasma, 15 L/min) was used with a 0.65 L/min sample uptake rate. The elements V, Fe, and Mn were measured using the wavelengths 292.464, 238.204, and 257.610 nm, respectively. Standard reference solutions purchased from Merck were used for calibration of the ICP-OES instrument. The compounds were dissolved in ICP-grade HNO_3 through acid digestion (2−3 times). After that, the clear HNO_3 solution of the material was calcined at 500 °C in a muffle furnace and the residue was dissolved in ICP-grade HNO_3 (1% v/v), filtered through 0.2 mm membrane, and used for analysis.

X-ray Crystallography. Diffraction-quality crystals of **1** (block, dark-brown crystals, 0.15 × 0.11 × 0.08 mm^3), **2** (block, brown crystals, 0.20 × 0.15 × 0.12 mm^3), **3** (block, dark-brown crystals, 0.39 × 0.35 × 0.16 mm^3), **5** (block, brown crystals, 0.18 × 0.15 × 0.10 mm^3), and **6** (block, dark-brown crystals, 0.23 × 0.19 × 0.17 mm^3) were collected from their respective reaction pots containing acetonitrile as the solvent. A crystal of compound **1** was mounted on a glass fiber without any protection, whereas those of compounds **2**, **3**, **5**, and **6** were coated with perfluoropolyether oil before mounting. Intensity data for the compounds were measured by employing a Bruker SMART APEX II CCD diffractometer equipped with a monochromatized Mo Kα radiation (λ = 0.71073 Å) source using the ω-scan technique at 298 K for compound **1** and at 150 K for compounds **2**, **3**, **5**, and **6**. No crystal decay was observed during data collection. The intensity data were corrected for empirical absorption. In all cases, absorption corrections based on multiscans using the *SADABS* software[20] were applied.

The structures were solved by direct methods[21] and refined on F^2 by a full-matrix least-squares procedure[22] based on all data minimizing R1 = $\sum||F_o| - |F_c||/\sum|F_o|$, wR2 = $[\sum[w(F_o^2 - F_c^2)^2]/\sum(F_o^2)^2]^{1/2}$, and $S = [\sum[w(F_o^2 - F_c^2)^2]/(n-p)]^{1/2}$. *SHELXL-97* was used for both structure solutions and refinements.[22] A summary of relevant crystallographic data and the final refinement details are given in Tables S1 and S2 (Supporting Information, SI). All non-hydrogen atoms were refined anisotropically. The hydrogen-atom positions were calculated and isotropically fixed in the final refinements [d(C−H) = 0.95 Å, with the isotropic thermal parameter of U_{iso}(H) = 1.2U_{iso}(C)]. In compound **2**, the oxygen-bound hydrogen atoms of the coordinated H_2O molecule have been located directly from the Fourier difference maps and refined isotropically with 100% site occupancy factors for each. The *SMART* and *SAINT-plus* software packages[23] were used for data collection and reduction, respectively. Crystallographic diagrams were drawn using the *DIAMOND* software package.[24] Unfortunately, the data sets for compounds **1** and **6** are incomplete in terms of the range of 2θ used in the refinements; the molecular structures, nevertheless, present no unusual features and have been determined unambiguously. We were unsuccessful in growing diffraction-grade crystals of compounds **4** and **7** in spite of our repeated attempts.

dx.doi.org/10.1021/ic501563r | Inorg. Chem. 2014, 53, 8287−8297

Scheme 2. Schematic Presentation for the Formation of Compounds 6 and 7[a]

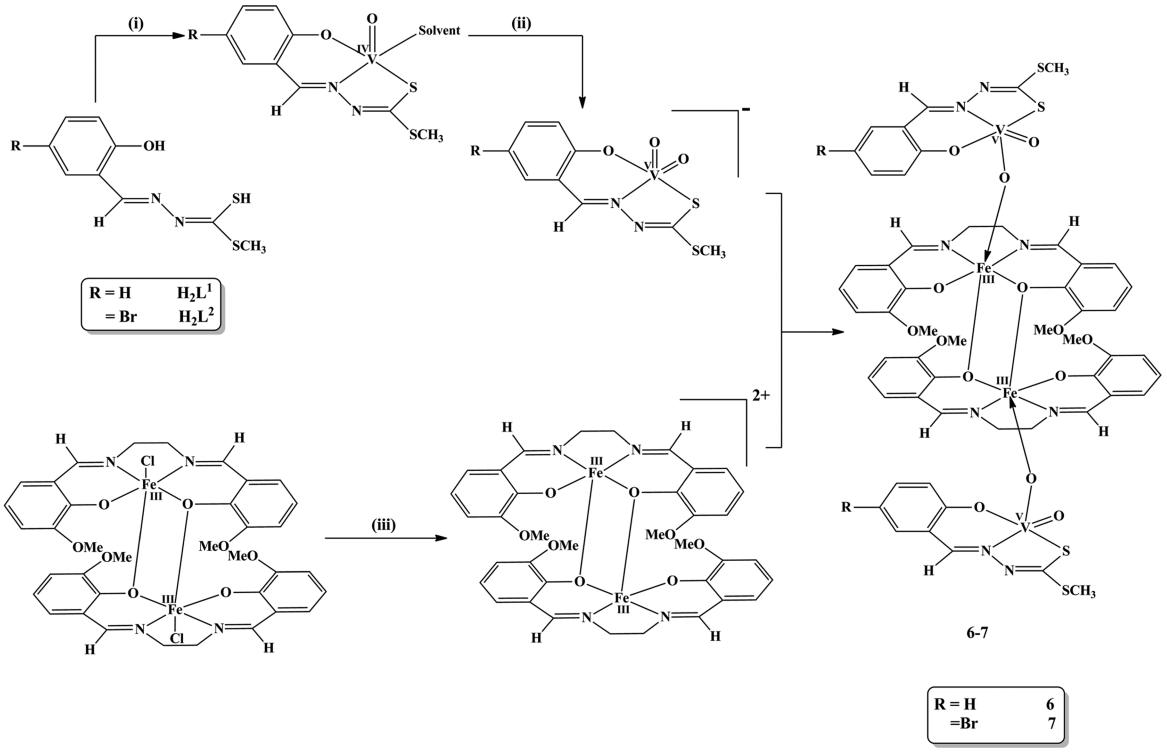

[a]Conditions: (i) $[VO(acac)_2]$ in acetonitrile; (ii) cation-assisted aerial oxidation; (iii) $AgNO_3/CH_3CN$.

RESULTS AND DISCUSSION

Syntheses. The heterobinuclear $[L'OV^V(\mu\text{-}O)Mn^{III}L]$ (**1**–**5**) and tetranuclear $[L'OV^V(\mu\text{-}O)Fe^{III}L]_2$ (**6** and **7**) compounds reported in this work involve discrete μ-oxido V^V-O-M^{III} (M = Mn, Fe) cores. The details of their syntheses are summarized in Schemes 1 and 2. When $[V^{IV}O(acac)_2]$ is allowed to react with the tridentate dithiocarbazate-based ligands (H_2L') in an acetonitrile solution under refluxing condition, a solvated species $[L'V^{IV}O(CH_3CN)]$ is initially formed. This species, as described elsewhere,[25] is aerially oxidized to a *cis*-dioxido anionic species $[L'V^VO_2]^-$ in the presence of an added cation. For the present series of compounds, we have used $[M^{III}L(H_2O)]^+$ (M = Mn, Fe; L^{2-} is a Salen-type N_2O_2 ligand) as the cationic species to induce the aerial oxidation of $[L'V^{IV}O(CH_3CN)]$ to anionic $[L'V^VO_2]^-$ species, which, in turn, is accommodated to one of the axial sites of $[M^{III}L(H_2O)]^+$ to generate the targeted compound $[L'OV^VOM^{III}L]$ (**1**–**7**). The cationic $[Mn^{III}L(H_2O)]^+$ species is generated in solution either by removing the coordinated chloro ligand from the $[M^{III}LCl]$ precursor using $AgNO_3$ as the reagent (for compounds **1**, **6**, and **7**) or by allowing $[Mn(OAc)_3]$ to react directly with H_2L in an acetonitrile solution[16a] (for compounds **2**–**5**).

The purities of these heterobimetallic compounds have been established by rigorous ICP-OES analyses of vanadium, manganese, and iron (summarized in the Experimental Section), which confirm a 1:1 V/M ratio in the reported compounds.

The IR spectra of complexes **1**–**7** are summarized in the Experimental Section. The compounds display several strong bands, characteristic of the coordinated ligands. These include a couple of strong bands appearing in the 1625–1597 and 1600–1508 cm^{-1} regions due to the ν(C=N) stretching modes of the Schiff-base moieties.[25,26] Also a prominent band in the 1301–1292 cm^{-1} region appears in all of these complexes due to ν(C–O/phenolate) stretching. The presence of a strong and sharp band in the 970–945 cm^{-1} region provides a signature for the terminal V=O_t stretching. Another interesting feature observed with these compounds is the appearance of a strong band in the 858–841 cm^{-1} region, which is possibly arising out of a stretched V=O bond,[27] forming part of the V=O → M (M = Mn or Fe) bridging moiety, as established by X-ray crystal structure analysis (see later).

Mass Spectrometry. ESI-MS data (in the positive-ion mode) for complexes **1**–**7** have been listed in the Experimental Section. Out of these, only compounds **1** and **2** display their molecular-ion peaks due to the $[M + Na]^+$ and $[M - H_2O - 2CH_3CN + Na]^+$ ionic species, respectively. The observed isotopic distributions and their simulation patterns are in agreement with these assigned formulations, as shown in Figures S1 and S2 (SI). The rest of the compounds appeared to be quite fragile under the conditions of ESI-MS and failed to provide the corresponding molecular-ion peaks. Interestingly, however, they all show the highest mass cluster corresponding to the breakdown product $[ML]^+$ (where M = Mn or Fe).

Description of the Crystal Structures. The molecular structures and atom-labeling schemes for compounds **1**–**3** and **6** are shown in Figures 1–4, respectively, and that of compound **5** is shown in Figure S3 (SI), providing confirmatory evidence in support of their discrete unsupported μ-oxido heterobinuclear (or tetranuclear for **6**) structures with unsymmetrical ligand environments. Their selected metrical parameters are summarized in Tables 1 and 2. Compounds **1** and **3** crystallize in the monoclinic space group $P2_1/c$ with four molecular mass units accommodated per unit cell. Compounds **2**, **5**, and **6**, on the other hand, have triclinic space group $P\bar{1}$ with two and four molecular mass units in compounds **2** and **5**, respectively, and one molecular mass unit in compound **6**, accommodated per unit

dx.doi.org/10.1021/ic501563r | Inorg. Chem. 2014, 53, 8287–8297

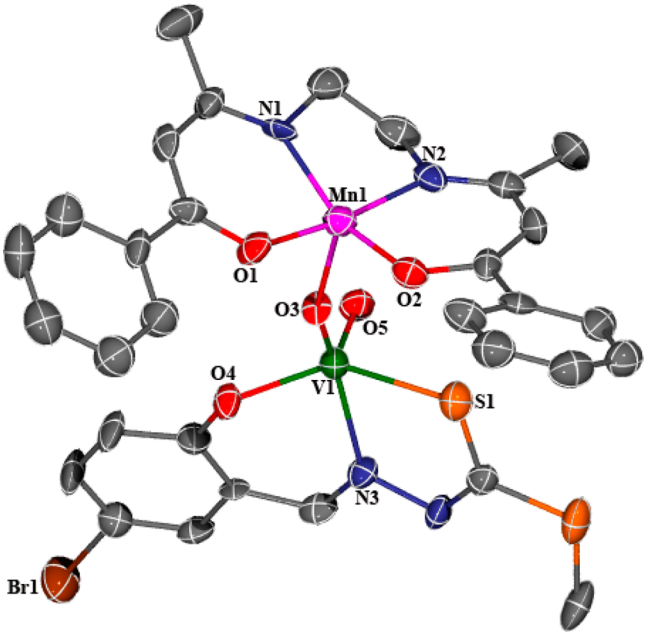

Figure 1. Molecular structure and atom-labeling scheme for compound **1** with thermal ellipsoids drawn at the 30% probability level. Hydrogen atoms have been omitted for clarity.

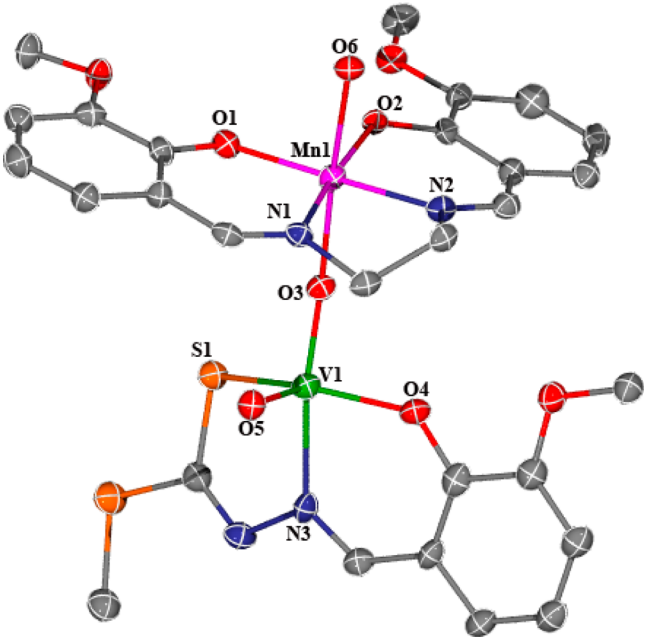

Figure 2. Molecular structure and atom-labeling scheme for compound **2** with thermal ellipsoids drawn at the 30% probability level. Hydrogen atoms and solvent molecules have been omitted for clarity.

cell. The manganese(III) centers in **1** and **3** are in a square-pyramidal environment (τ = 0.25 and 0.13, respectively),[28] with O1, N1, N2, and O2 donor atoms from the tetradentate ligands (L^4 and L^6) forming the basal plane while the apical position is filled by the bridging oxido atom O3. In compounds **2** and **5**, the coordination geometry around the manganese(III) centers is octahedral. The basal positions are completed by O1, N1, N2, and O2 donor atoms, all coming from the tetradentate ligands (L^5 and L^8), while the axial positions are taken up by a coordinated water molecule, O6, along with the bridging oxido atom O3. The iron(III) centers in compound **6** are octahedral. Here the basal positions are occupied by O1, N1, N2, and O2 donor atoms, whereas the axial positions are occupied by the bridging O3 atom and a bridging aryloxido O1# atom from another L^5Fe moiety, thus forming a dimeric structure. The trans angles O3−Mn1−O6 173.64(16)° [173.2(3)° for **5**], O1−Mn1−N2 173.3(2)° [173.9(3)°], and O2−Mn1−N1 173.7(2)° [173.9(4)°] are close to linearity in compounds **2** and **5**, as expected for an octahedral geometry. The latter two angles in **1** and **3**, 155.3(3)° [174.4(8)° for **3**] and 170.6(3)° [166.6(8)°], are, however, slightly compressed, characteristic of a square pyramid with a flattened base. The trans angles O3−Fe1−O1# 172.5(2)°, O1−Fe1−N2 158.7(3)°, and O2−Fe1−N1 165.3(3)° in compound **6** are slightly compressed probably because of the bridging nature of the coordinating aryloxido atom. The average M−O and M−N (M = Fe, Mn) distances in the basal plane are in the expected range.[29] The apical Mn−O distances Mn1−O3 [2.042(5)−2.211(7) Å] and Mn1−O6 [2.257(6)−2.284(5) Å], on the other hand, are significantly enlarged because manganese(III) is a Jahn−Teller ion.[30]

The coordination geometry around the vanadium(V) centers in all of the above four structures in **1**−**3** and **5** is square-pyramidal. While the vanadium center in **5** is a perfect square pyramid (τ = 0), others show distortion of variable degrees (τ in the range 0.21−0.13). The vanadium centers in the tetranuclear complex **6** are also square-pyramidal with marginal distortions (τ = 0.06 and 0.12, respectively). The donor atoms O4, N3, and S1 from the tridentate dithiocarbazate-based ligands (L′ = L^1−L^3) complete the equatorial sites along with the bridging oxido atom O3, while the sole apical site is taken up by the terminal oxido atom O5. The trans angles here, O3−V1−N3 and O4−V1−S1, vary in the ranges 153.2(3)−144.91(9)° and 151.92(6)−140.6(2)°, respectively, and are much shorter of linearity, providing indications of distortion in the meridian plane and accounting for large displacement of the V1 atom from the least-squares basal plane by 0.54, 0.52, 0.51, 0.48, and 0.50 Å in compounds **1**−**3**, **5**, and **6**, respectively, toward the apical oxido atom O5. The V−O, V−N, and V−S distances are all in the expected range.[7]

The metal centers in these compounds are connected by an unsupported bridging oxido atom, O3. Interestingly, the V1−O3 [1.664(9)−1.711(6) Å] and M1−O3 (M = Mn or Fe) distances [2.211(7)−1.943(6) Å] that are parts of this bridge differ widely in these molecules. In fact, the V1−O3 distances are close to that of a V═O double bond, while the M1−O3 (M = Mn^{III} or Fe^{III}) distances are much more elongated compared to a M^{III}−O single bond. Therefore, it is prudent to represent the electronic structure of the V−O−M oxido bridge in these compounds by the canonical structure V═O → M.[6] Of particular interest in these structures also is the V−O−Mn bridging angle, which shows systematic variation due to the changes in the dihedral angle (summarized in Table 3), between the basal planes surrounding the metal centers, with the latter being controlled by steric congestion in the ligand backbones. The change in the bridging angle has a direct, albeit moderate, impact on the V···Mn separation, which changes from 3.637 to 3.493 Å on going from **1** to **5**. On the other hand, in the case of the remaining compound **6**, the two iron centers are separated by 3.261 Å. The Fe···V separation is 3.50 Å, and the dihedral angle between the basal planes surrounding the metal centers is 70.73°.

Interestingly, compounds **2** and **5** have dimeric structures in the solid state due to their association through intermolecular hydrogen bonding, as summarized in Table S3 (SI). A representative dimeric structure for **2** is displayed in Figure 5,

dx.doi.org/10.1021/ic501563r | Inorg. Chem. 2014, 53, 8287−8297

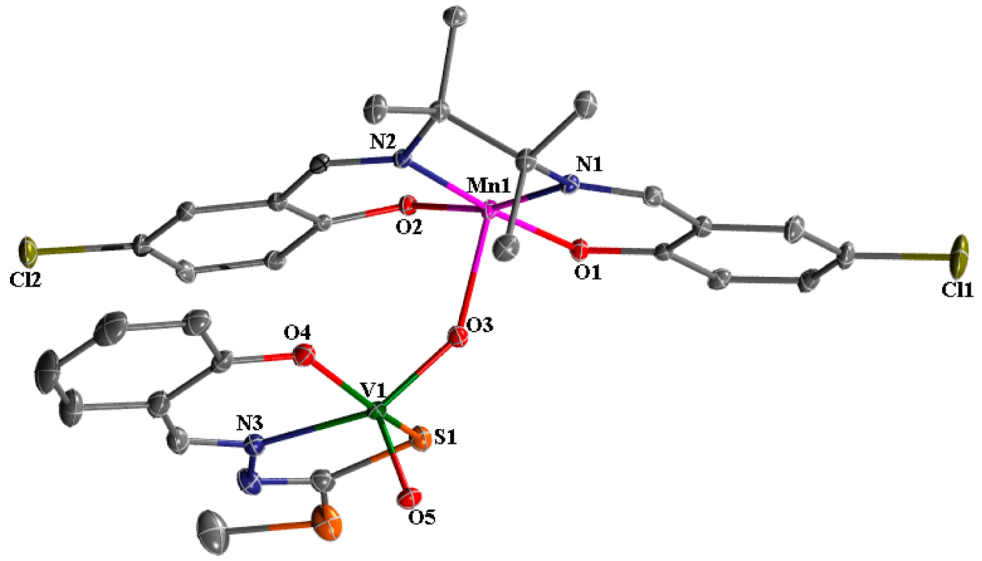

Figure 3. Molecular structure and atom-labeling scheme for compound **3** with thermal ellipsoids drawn at the 30% probability level. Hydrogen atoms have been omitted for clarity.

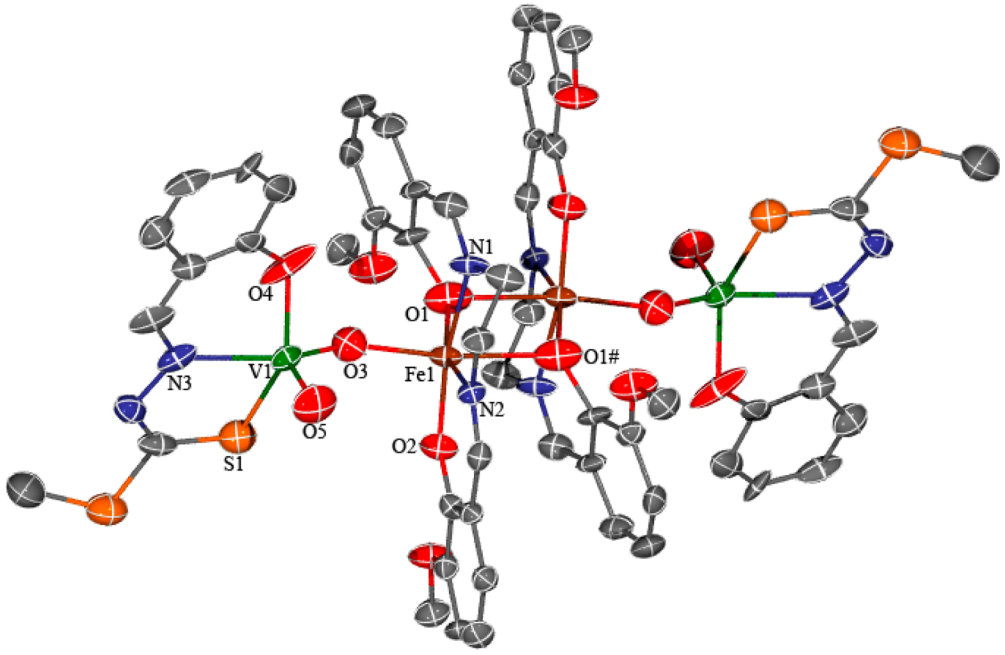

Figure 4. Molecular structure and atom-labeling scheme for compound **6** with thermal ellipsoids drawn at the 30% probability level. Hydrogen atoms and solvent molecule have been omitted for clarity.

in which two molecules of the compound are connected head to head by hydrogen bonding. The H6A and H6B atoms of the coordinated H_2O molecule attached to the manganese center are each connected to a phenolate oxygen (O1 and O2) and the methoxy oxygen atoms (O7 and O8) of the partner molecule such that O6−H6A···O2, 2.889 Å (143.02°); O6−H6A···O8, 2.989 Å (147.80°); O6−H6B···O1, 2.939 Å (142.19°); and O6−H6B···O7, 2.916 Å (143.62°), as labeled in Figure 5, are close to linearity. The observed data suggest reasonably strong hydrogen bonding between the two neighboring molecules in **2**, thus providing a dimeric structure in the solid state.

^{51}V NMR Spectroscopy. In order to understand more about the solution structures of these heterobimetallic compounds, the ^{51}V NMR spectra of **1**−**5** have been recorded in dimethyl sulfoxide (DMSO)-d_6. Compound **1** shows a single sharp signal at −455 ppm. For compounds **2**−**5**, the corresponding signal appears within a narrow range in a slightly downfield region at −465, −467, −462, and −464 ppm, respectively. Spectra for compounds **1** and **3** are displayed in Figures S4 and S5 (SI), respectively, as representative examples. The appearance of a solitary signal actually confirms the purity of these heterobimetallic compounds involving a single vanadium center. These data also indicate that the electronic environment surrounding the vanadium center in **1** is somewhat different from those in the rest of these molecules. This is not unlikely considering that the tetradentate ligand around the manganese center in **1** is a Schiff base of a β-diketonate-type molecule, which is replaced in **2**−**5** by Salen-type ligands, responsible for generating structural differ-

dx.doi.org/10.1021/ic501563r | *Inorg. Chem.* 2014, 53, 8287−8297

Table 1. Selected Bond Distances and Angles for Compounds 1−3 and 5

	1	2	3	5
Bond Distances (Å)				
Mn1−O1	1.896(7)	1.878(4)	1.8847(17)	1.874(7)
Mn1−O2	1.870(6)	1.882(4)	1.9108(17)	1.877(7)
Mn1−O3	2.042(5)	2.138(4)	2.1158(18)	2.211(7)
Mn1−N1	1.948(8)	1.976(5)	1.992(2)	1.974(9)
Mn1−N2	1.967(8)	1.972(5)	1.997(2)	1.972(9)
V1−O3	1.678(5)	1.665(4)	1.6865(18)	1.664(9)
V1−O4	1.923(6)	1.909(5)	1.9145(19)	1.886(10)
V1−O5	1.617(6)	1.629(4)	1.6086(18)	1.590(7)
V1−N3	2.148(8)	2.181(6)	2.159(2)	2.170(13)
V1−S1	2.370(3)	2.363(2)	2.4072(8)	2.366(5)
Mn1−O6		2.284(5)		2.257(6)
Bond Angles (deg)				
	1	2	3	5
O1−Mn1−O2	89.0(3)	93.40(18)	92.43(7)	93.2(3)
O1−Mn1−O3	102.5(2)	94.05(17)	92.75(7)	88.1(3)
O2−Mn1−O3	94.5(3)	92.78(17)	96.70(7)	89.4(3)
O1−Mn1−N1	90.6(4)	92.4(2)	93.77(8)	92.8(4)
O2−Mn1−N1	170.6(3)	173.7(2)	166.60(8)	173.9(4)
O1−Mn1−N2	155.3(3)	173.3(2)	174.40(8)	173.9(3)
O2−Mn1−N2	91.1(4)	91.40(19)	91.58(8)	92.9(3)
N2−Mn1−N1	85.3(4)	82.6(2)	81.52(8)	81.1(4)
N1−Mn1−O3	94.7(3)	89.25(19)	94.87(7)	90.2(3)
N2−Mn1−O3	102.2(3)	90.35(19)	90.66(8)	92.6(3)
O5−V1−O3	109.9(3)	108.5(2)	108.64(10)	108.5(4)
O5−V1−O4	108.0(3)	107.5(2)	104.51(9)	105.0(4)
O3−V1−O4	97.9(3)	95.25(19)	96.29(8)	96.6(4)
O5−V1−N3	95.6(3)	97.8(2)	105.20(9)	102.5(4)
O3−V1−N3	153.2(3)	152.7(2)	144.91(9)	148.2(4)
O4−V1−N3	81.6(3)	83.33(19)	83.87(8)	82.2(4)
O5−V1−S1	107.0(2)	105.02(16)	100.86(7)	102.8(3)
O3−V1−S1	86.8(2)	88.60(15)	86.74(6)	89.0(3)
O4−V1−S1	140.6(2)	144.10(15)	151.92(6)	148.2(3)
N3−V1−S1	77.4(3)	77.48(14)	78.01(6)	76.9(4)
N4−N3−V1	124.3(6)	120.9(4)	122.69(17)	123.2(11)
V1−O3−Mn1	155.3(3)	145.7(2)	141.39(11)	128.1(5)
O3−Mn1−O6		173.64(16)		173.2(3)

ences in the vanadium(V) coordination sphere, as reflected in their ^{51}V NMR spectra.

Electrochemistry. Cyclic voltammograms of compounds **1**−**7** have been recorded at a glassy carbon working electrode under an atmosphere of purified dinitrogen in a DMF solution (0.1 M TBAP) at 25 °C in the potential range of −2.5 to +0.5 V vs Ag/AgCl reference, and the results are summarized in Table 4. The voltammetric features are quite similar for compounds **1**−**5**, each displaying three electrochemical responses, all in the cathodic region, as shown in Figures S6 (SI) and 6 for two representative compounds **1** and **2**, respectively. These include, in the CV of compound **2**, a reversible process at $(E_{1/2})_I = -0.17$ V ($\Delta E_p = 60$ mV, process I), an irreversible process at $E_{pc} = -1.70$ V (process II), and a second reversible process at $(E_{1/2})_{II} = -1.83$ V ($\Delta E_p = 60$ mV, process III). The corresponding processes in **1** appear at −0.32 V ($\Delta E_p = 80$ mV) and −1.68 and −1.83 V ($\Delta E_p = 60$ mV), respectively, and each appears to be cathodic, as judged by steady-state voltammetry. Unfortunately, the electron stoichiometry determinations for these couples by constant potential coulometric experiments have failed with all of these compounds because of the instability of the reduction products

Table 2. Selected Bond Distances and Angles for Compound 6

Bond Distances (Å)			
Fe1−O2	1.872(6)	V1−O5	1.590(6)
Fe1−O3	1.943(6)	V1−O3	1.711(6)
Fe1−O1	1.944(6)	V1−O4	1.953(8)
Fe1−N2	2.061(8)	V1−N3	2.219(9)
Fe1−N1	2.111(8)	V1−S1	2.335(4)
Fe1−O1#	2.244(7)		
Bond Angles (deg)			
O2−Fe1−O3	96.7(3)	N2−Fe1−O1#	87.9(3)
O2−Fe1−O1	106.8(3)	N1−Fe1−O1#	83.5(3)
O3−Fe1−O1	97.7(3)	O5−V1−O3	110.1(3)
O2−Fe1−N2	88.9(3)	O5−V1−O4	104.8(3)
O3−Fe1−N2	94.6(3)	O3−V1−O4	94.5(3)
O1−Fe1−N2	158.7(3)	O5−V1−N3	97.6(3)
O2−Fe1−N1	165.3(3)	O3−V1−N3	151.3(3)
O3−Fe1−N1	90.1(3)	O4−V1−N3	85.1(3)
O1−Fe1−N1	85.1(3)	O5−V1−S1	104.2(3)
N2−Fe1−N1	77.5(3)	O3−V1−S1	88.5(2)
O2−Fe1−O1#	90.4(2)	O4−V1−S1	147.7(3)
O3−Fe1−O1#	172.5(2)	N3−V1−S1	77.3(3)
O1−Fe1−O1#	77.9(3)	V1−O3−Fe1	146.1(4)

Table 3. Comparison between the V−O−Mn Bridge Angles and the Dihedral Angles (between the Basal Planes) in the V−O−Mn Compounds

	1	2	3	5
V−O−Mn bridge angle (deg)	155.3	145.7	142.3	128.1
dihedral angle (deg) between the basal planes	86.82	73.69	33.02	20.92

(obtained during electrolysis) in the longer time scale of the coulometric experiments. The results of normal-pulse voltammetry (NPV) experiments, also shown in Figures 6 and S6 (SI), however indicate the involvement of an identical number of electron(s) in each of these reduction processes. Further, on the basis of a comparison with the Fc/Fc$^+$ couple ($\Delta E_p = 70$ mV),[19] measured under identical experimental conditions, these processes appear to be monoelectronic.

Because both manganese(III) and vanadium(V) centers are electroactive, as are the Salen-type ligands,[31] we have decided to record the voltammograms of the precursor compounds [L^4 Mn^{III}Cl] and [L^5 Mn^{III}(H$_2$O)]ClO$_4$ as control under conditions identical with those of compounds **1**−**5** in order to decide if any one or more of the above three electron transfer(s) are based on Mn^{III}. The voltammograms are displayed in the insets of Figures S6 (SI) and 6, respectively, which involve, in each case, a reversible process at $E_{1/2} = -0.19$ V (−0.34 V for [L^4 Mn^{III}Cl]) for Mn^{III}/Mn^{II} reduction together with an irreversible reduction at $E_{pc} = -2.31$ V (−2.42 V), probably based on the attached tetradentate ligand. Taking a cue from these experiments, we now feel confident enough to conclude that process I above is a reduction process based on a Mn^{III}/Mn^{II} electron transfer, process II is possibly a ligand-based process, and process III is a vanadium-based V^{V}O/V^{IV}O electron transfer, as established earlier.[10] The electrochemical results of compounds **1**−**5** thus indicate the possible involvements of three heterobimetallic species with oxidation state combinations, shown by eqs 1 and 2.

$$[L'OV^{V}OMn^{III}L] \underset{(E_{1/2})_I}{\overset{+e^-}{\rightleftharpoons}} [L'OV^{V}OMn^{II}L]^- \quad (1)$$

dx.doi.org/10.1021/ic501563r | Inorg. Chem. 2014, 53, 8287−8297

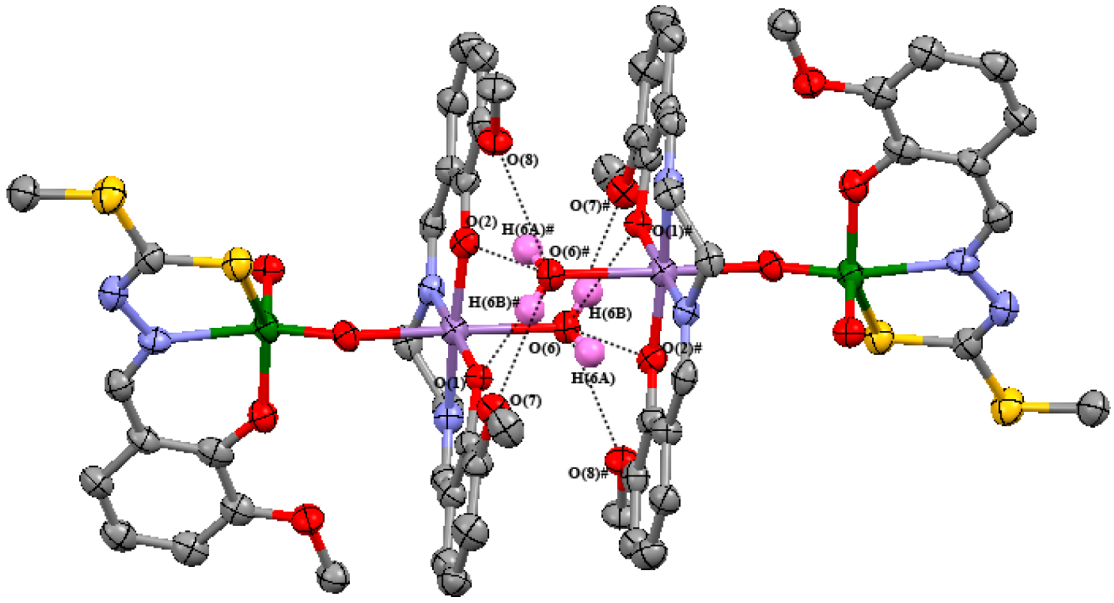

Figure 5. Intermolecular hydrogen-bonding interactions observed in compound **2**.

Table 4. Summary of the Electrochemical Data[a]

	process I		process II	process III	
compound	$(E_{1/2})_I$/V[b]	ΔE_p[c]/mV	E_{pc}/V	$(E_{1/2})_{II}$/V	ΔE_p/mV
1	−0.32	80	−1.68	−1.83	60
2	−0.17	60	−1.70	−1.83	60
3	−0.05	90	−1.65	−1.82	90
4	−0.06	120	−1.68	−1.81	80
5	−0.13	100	−1.64	−1.80	80

[a]All potentials vs Ag/AgCl reference. [b]$E_{1/2} = (E_{pc} + E_{pa})/2$. [c]$\Delta E_p = E_{pc} \sim E_{pa}$ at a scan rate of 100 mV/s.

$$[L'OV^{V}OMn^{II}L]^{1-} \underset{(E_{1/2})_{II}}{\overset{+e^-}{\rightleftharpoons}} [L'OV^{IV}OMn^{II}L]^{2-} \quad (2)$$

The voltammograms for the tetranuclear complexes **6** and **7** are much more complicated but, nevertheless, closely similar to each other. The CV for **6** (Figure 7) will be described as a representative example that involves at least four irreversible processes, all in the cathodic range, appearing at E_{pc} = −0.20, −1.0, −1.58, and −1.68 V (processes IV−VII) together with a reversible process (process VIII) at $E_{1/2}$ = −1.80 V (ΔE_p = 80 mV). Corresponding redox processes with compound **7** appear at −0.22, −0.98, −1.58, −1.65, and −1.79 V (ΔE_p = 80 mV), respectively. Once again, we checked the voltammogram of the precursor compound $[L^5FeCl]_2$ as a control to understand the origin of these electron-transfer processes. The control cyclic voltammogram, shown in the potential range of +0.3 to −2.1 V (Figure S7, SI), involves two reversible processes both in the cathodic region at $E_{1/2}$ = −0.24 and −1.68 V with ΔE_p = 80 and 70 mV, respectively, together with an irreversible spike at −1.62 V. The corresponding normal-pulse voltammogram, also displayed in Figure S7 (SI), indicates that both of the reversible processes involve identical numbers of electron(s). Comparison with a Fc/Fc^+ couple as an internal standard (ΔE_p = 70 mV; i_{pc}/i_{pa} = 1.0 at 100 mV/s) gives an indication that these couples are monoelectronic. We believe that the reduction at $E_{1/2}$ = −0.24 mV is due to a Fe^{III}/Fe^{II} reduction and the remaining reductions at higher cathodic potentials are due to ligand-based processes, in line with the arguments given earlier for compounds **1**−**5**. Taking

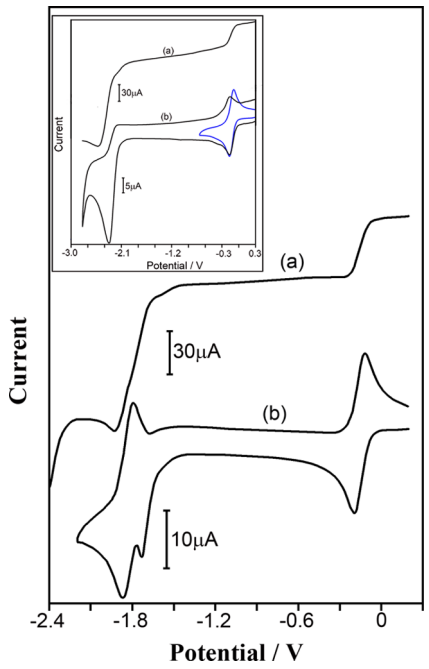

Figure 6. (a) Normal-pulse and (b) cyclic voltammograms of compound **2** in DMF: potentials vs Ag/AgCl; 0.1 M TBAP at a glassy carbon working electrode; scan rate of 100 mV/s. Inset: (a) NPV and (b) CV of the precursor compound $[L^5\ Mn^{III}(H_2O)]ClO_4$ under identical conditions.

a cue from these results, one can argue that processes IV and V at E_{pc} = −0.20 and −1.0 V, respectively, in the voltammogram of **6** are both due to Fe^{III}/Fe^{II} reductions, each involving an iron(III) center in this tetranuclear compound, while the remaining irreversible processes VI and VII at E_{pc} = −1.58 and −1.68 V are based on the ligands. The reversible process VIII at $E_{1/2}$ = −1.80 V is most likely due to a VO^{3+}/VO^{2+} reduction along with some contributions from the ligand-based reduction(s).[31] Coulometric confirmations of electron stoichiometry for these processes were not possible for the reasons already cited for compounds **1**−**5**. However, current height data from the NPV experiments (also

dx.doi.org/10.1021/ic501563r | Inorg. Chem. 2014, 53, 8287−8297

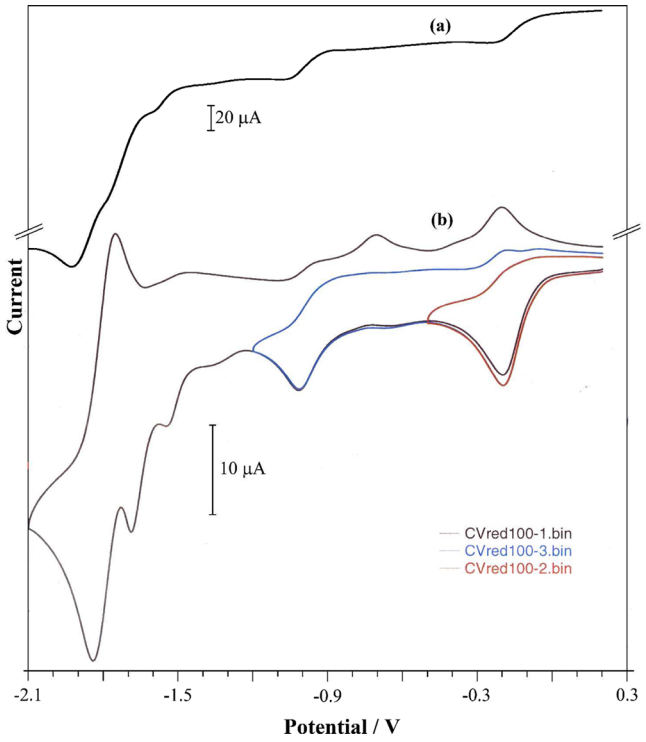

Figure 7. (a) Normal-pulse and (b) cyclic voltammograms of **6** in DMF: potentials vs Ag/AgCl; 0.1 M TBAP at a glassy carbon working electrode; scan rate of 100 mV/s.

shown in Figure 7) indicate identical electron stoichiometry for processes IV and V. Unlike in the precursor compound, the electron transfers in the iron(III) centers in **6** and **7** are irreversible at slower scan rates. The reduced iron(II) species are not stable enough to appear in the reverse scan of CV at 100 mV/s. At a very high scan rate (ν > 1000 mV/s), however, the reduced species do survive to appear as a quasi-reversible voltammogram, as shown in Figure 8 for process IV with compound **6**. In summary, the redox behavior of the tetranuclear $[V^{V}OFe^{III}]_2$ compounds is much more complex because of their instability

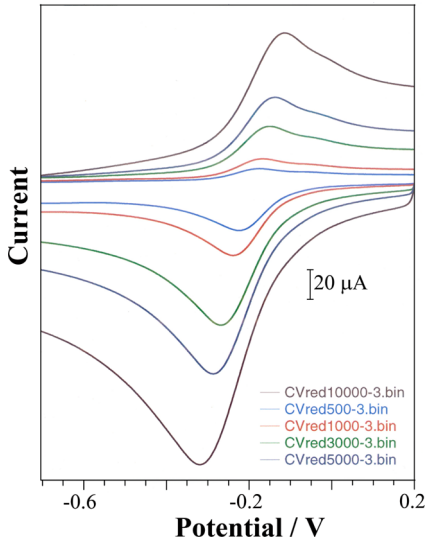

Figure 8. Cyclic voltammograms of compound **6** at high scan rates (500, 1000, 3000, 5000, and 10000 mV/s) in DMF: potentials vs Ag/AgCl; 0.1 M TBAP at a glassy carbon working electrode.

even in the shorter time scale of the CV experiments. Nevertheless, they do show a similar trend in their electrochemical behavior, which includes both metal-based (Fe^{III}/Fe^{II} and VO^{3+}/VO^{2+}) and ligand-based reductions.

Reactivity Study. Syntheses of cationic oxidovanadium(V) complexes $[L'OV^{V}]^{+}$ via the abstraction of a bridging oxido ligand from the μ-oxidovanadium(V) compounds (**1**−**7**) have been attempted following a reported procedure[32] using $[Et_3SiH][CF_3SO_3]$ as the oxo-abstracting reagent. Such cationic complexes are widely used in many catalytic processes. Reactions at refluxing temperature in a dichloromethane solution using these complexes and the hydrosilylating reagent in a 1:2 mol ratio have failed to generate any product, thus confirming the V^{V}−O−M^{III} moiety to be kinetically inert, as observed with compounds having a Re^{V}−O−Re^{V} bridge.[33]

Comparison with Compounds Containing a $[V_2O_3]^{n+}$ Core. A comparison between the structural and physicochemical properties of the present series of heterobimetallic compounds (**1**−**7**) with those of the μ-oxidodivanadium compounds containing $[V_2O_3]^{n+}$ (n = 4, 3, and 2) cores sounds prudent at this stage. When both the vanadium centers of these $[V_2O_3]^{n+}$ cores have octahedral geometry, the molecules in most of the cases have a linear V−O−V bridge with terminal oxido groups in mutually trans positions.[5t,v] On the other hand, when the vanadium centers are both five-coordinate having square-pyramidal geometry, a V−O−V bridge appears to be angular with terminal oxido groups having diverse types of arrangements, featuring anti-linear[5n,o] to syn-angular[5p,7,8] through anti-angular[5c,e,j] and twist-angular[5u] structures. The bridging V−O_b distances in these homobinuclear compounds are generally similar,[5] barring a few trapped-valency compounds with the $[V_2O_3]^{3+}$ core in which disparate V−O_b bonds (1.76 vs 1.83 Å)[7] are reported. Interestingly, when asymmetry is introduced into the coordination geometry surrounding the vanadium centers that comprise the V_2O_3 core,[5g,9,10] the V−O−V bridge becomes once again angular, with the bridge angle varying in a wider range (166.20−117.92°) depending upon the steric congestion provided by the ligands.[5g,10] Besides a lone exception,[5g] a large amount of disparity is observed between the V−O bonds (1.65 vs 2.17 Å)[10] that make the V−O−V bridge in these asymmetric compounds. Inequality to a large extent is also observed between the V−O and M−O distances that make up the V−O−M bridges in the present series of heterobimetallic compounds (**1**−**7**). Electrochemically, also these heterobinuclear compounds, like their homodinuclear counterparts, are redox-active, all undergoing a $V^{V/IV}$ reduction with different degrees of reversibility. The former compounds, in addition, undergo further reduction(s) involving the heterometal (Mn^{3+}, Fe^{3+}) centers of these V^{V}−O−M^{III} cores.

CONCLUSIONS

Syntheses of μ-oxido heterobinuclear compounds (**1**−**7**) containing discrete $[V^{V}$−O−$M^{III}]_n$ (n = 1, M = Mn; n = 2, M = Fe) cores have been reported through a targeted synthesis route. The identities of these compounds have been conclusively established by ESI-MS and single-crystal X-ray diffraction analysis. The latter analyses have proved conclusively that the μ-oxido group in these compounds exists more like in a V═O → M canonical form. The dihedral angle between the basal planes surrounding the metal centers controls the V−O−M bridge angle, which varies in the range 128.1−155.3° in compounds **1**−**5**. In the tetranuclear complexes **6** and **7**, the binuclear units are connected by a pair of aryloxido linkers, forming a pair of Fe^{III}−

dx.doi.org/10.1021/ic501563r | Inorg. Chem. 2014, 53, 8287−8297

O−Fe^{III} bridges. The metal centers in these heterometallic cores are redox-active, undergoing one-electron reductions involving M^{III}/M^{II} and $V^{V}O/V^{IV}O$ electron transfers, as judged by CV and NPV experiments. The electron transfer at the manganese(III) centers in compounds **1**−**5** is reversible, unlike in the tetranuclear compounds **6** and **7**, where the electron transfers at the iron(III) centers are irreversible at slower scan rates (viz. 100 mV/s) but improve to reversibility when the scan rate is increased to ca. 1000 mV/s or more.

■ ASSOCIATED CONTENT

Supporting Information

Summary of relevant X-ray crystallographic data for compounds **1**−**3**, **5**, and **6** (Tables S1 and S2), hydrogen-bond geometry of compounds **2** and **5** (Table S3), ESI-MS spectra of compounds **1** and **2** (Figures S1 and S2), molecular structure of compound **5** (Figure S3), ^{51}V NMR spectra of compounds **1** and **3** (Figures S4 and S5), CV and NPV of compounds **1** and $[L^{5}FeCl]_2$ (Figures S6 and S7), and X-ray crystallographic files in CIF format for compounds **1**−**3**, **5**, and **6**. This material is available free of charge via the Internet at http://pubs.acs.org.

■ AUTHOR INFORMATION

Corresponding Author

*E-mail: icmc@iacs.res.in.

Notes

The authors declare no competing financial interest.

■ ACKNOWLEDGMENTS

This work was supported by the Council of Scientific and Industrial Research (CSIR), New Delhi, India. K.B., S.M.T.A., and M.C.M. also thank the CSIR for the award of research fellowships. The single-crystal X-ray diffraction data were recorded on an instrument supported by DST, New Delhi, India, as a National Facility at IACS under the IRHPA program. We are indebted to Dr. P. Paul and Dr. P. B. Chatterjee of CSIR-CSMCRI, Bhavnagar, India, for their help in completing the ICP-OES analyses of the samples and Professor E. R. T. Tiekink of the University of Malaya for helpful discussions.

■ REFERENCES

(1) (a) Singh, S.; Roesky, H. W. *Dalton Trans.* **2007**, 1360. (b) Bottomley, F.; Goh, S.-K. *Polyhedron* **1996**, *15*, 3045. (c) West, B. O. *Polyhedron* **1989**, *8*, 219.

(2) Lippard, S. J.; Berg, J. M. *Principles of Bioinorganic Chemistry*; University Science Books: Sausalito, CA, 1994.

(3) See for example: (a) Kim, E.; Chufán, E. E.; Kamaraj, K.; Karlin, K. D. *Chem. Rev.* **2004**, *104*, 1077 and references cited therein. (b) Gurubasavaraj, P. M.; Mandal, S. K.; Roesky, H. W.; Oswald, R. B.; Pal, A.; Noltemeyer, M. *Inorg. Chem.* **2007**, *46*, 1056. (c) Bai, B.; Singh, S.; Roesky, H. W.; Noltemeyer, M.; Schmidt, H.-G. *J. Am. Chem. Soc.* **2005**, *127*, 3449. (d) Schulz, L. D.; Fallon, G. D.; Moubaraki, B.; Murray, K. S.; West, B. O. *J. Chem. Soc., Chem. Commun.* **1992**, 971.

(4) The Seventh International Symposium on the Chemistry and Biological Chemistry of Vanadium. In *Coordination Chemistry Reviews*; Michibata, H., Kanamori, K., Hirao, T., Eds.; Elsevier BV: Amsterdam, The Netherlands, 2011; Vol. *255*, p 2149.

(5) See for example: (a) Avecilla, F.; Adão, P.; Correia, I.; Pessoa, J. C. *Pure Appl. Chem.* **2009**, *81*, 1297. (b) Knopp, P.; Wieghardt, K.; Nuber, B.; Weiss, J.; Sheldrick, W. S. *Inorg. Chem.* **1990**, *29*, 363. (c) Bellemin-Laponnaz, S.; Coleman, K. S.; Dierkes, P.; Masson, J. P.; Osborn, J. A. *Eur. J. Inorg. Chem.* **2000**, 1645. (d) Nielsen, K.; Rasmus, R.; Eriksen, K. M. *Inorg. Chem.* **1993**, *32*, 4825. (e) Dutta, S.; Basu, P.; Chakravorty, A. *Inorg. Chem.* **1993**, *32*, 5343. (f) Knopp, P.; Wieghardt, K.; Nuber, B.; Weiss, J.; Sheldrick, W. S. *Inorg. Chem.* **1990**, *29*, 363. (g) Nicolakis, V. A.; Stathopoulos, P.; Exarchou, V.; Gallos, J. K.; Kubicki, M.; Kabanos, T. A. *Inorg. Chem.* **2010**, *49*, 52. (h) Toftlund, H.; Larsen, S.; Murray, K. S. *Inorg. Chem.* **1991**, *30*, 3964. (i) Maurya, M. R.; Kumar, A.; Bhat, A. R.; Azam, A.; Bader, C.; Rehder, D. *Inorg. Chem.* **2006**, *45*, 1260. (j) Dinda, R.; Sengupta, P.; Ghosh, S.; Mak, T. C. W. *Inorg. Chem.* **2002**, *41*, 1684. (k) Adão, P.; Pessoa, J. C.; Henriques, R. T.; Kuznetsov, M. L.; Avecilla, F.; Maurya, M. R.; Kumar, U.; Correia, I. *Inorg. Chem.* **2009**, *48*, 3542. (l) Nishizawa, M.; Hirotsu, K.; Ooi, S.; Saito, K. *J. Chem. Soc., Chem. Commun.* **1979**, 707. (m) Schulz, D.; Weyhermüller, T.; Wieghardt, K.; Nuber, B. *Inorg. Chim. Acta* **1995**, *240*, 217. (n) Wang, D.; Behrens, A.; Farahbakhsh, M.; Gatjens, J.; Rehder, D. *Chem.—Eur. J.* **2003**, *9*, 1805. (o) Pessoa, J. C.; Calhorda, M. J.; Cavaco, I.; Correio, I.; Duarte, M. T.; Felix, V.; Henriques, R. T.; Piedade, M. F. M.; Tomaz, I. *J. Chem. Soc., Dalton Trans.* **2002**, 4407. (p) Pessoa, J. C.; Silva, J. A. L.; Vieira, A. L.; Vilas-Boas, L.; O'Brien, P.; Thronton, P. *J. Chem. Soc., Dalton Trans.* **1992**, 1745. (q) Chakravarty, J.; Dutta, S.; Chakravorty, A. *J. Chem. Soc., Dalton Trans.* **1993**, 2857. (r) Kojima, A.; Okazaki, K.; Ooi, S.; Saito, K. *Inorg. Chem.* **1983**, *22*, 1168. (s) Launay, J.-P.; Jeannin, Y.; Daoudi, M. *Inorg. Chem.* **1985**, *24*, 1052. (t) Ghosh, S.; Nanda, K. K.; Addison, A. W.; Butcher, R. J. *Inorg. Chem.* **2002**, *41*, 2243. (u) Mondal, S.; Ghosh, P.; Chakravorty, A. *Inorg. Chem.* **1997**, *36*, 59. (v) Holwerda, R. A.; Whittlesey, B. R.; Nilges, M. *Inorg. Chem.* **1998**, *37*, 64. (w) Mahroof-Tahir, M.; Keramidas, A. D.; Goldfarb, R. B.; Anderson, O. P.; Miller, M. M.; Crans, D. C. *Inorg. Chem.* **1997**, *36*, 1657. (x) Mondal, A.; Sarkar, S.; Chopra, D.; Guru Row, T. N.; Pramanik, K.; Rajak, K. K. *Inorg. Chem.* **2005**, *44*, 703.

(6) (a) Bossek, U.; Knopp, P.; Habenicht, C.; Wieghardt, K.; Nuberb, N.; Weiss, J. *J. Chem. Soc., Dalton Trans.* **1991**, 3165. (b) Mazzanti, M.; Chiesi-Villa, A.; Guastini, C. *Inorg. Chem.* **1986**, *25*, 4158.

(7) Dutta, S. K.; Kumar, S. B.; Bhattacharyya, S.; Tiekink, E. R. T.; Chaudhury, M. *Inorg. Chem.* **1997**, *36*, 4954.

(8) Dutta, S. K.; Samanta, S.; Kumar, S. B.; Han, O. H.; Burckel, P.; Pinkerton, A. A.; Chaudhury, M. *Inorg. Chem.* **1999**, *38*, 1982.

(9) Chatterjee, P. B.; Kundu, N.; Bhattacharya, S.; Choi, K.-Y.; Endo, A.; Chaudhury, M. *Inorg. Chem.* **2007**, *46*, 5483.

(10) Chatterjee, P. B.; Bhattacharya, S.; Audhya, A.; Choi, K.-Y.; Endo, A.; Chaudhury, M. *Inorg. Chem.* **2008**, *47*, 4891.

(11) A part of this work has been published as a rapid communication: Bhattacharya, K.; Maity, M.; Mondal, D.; Endo, A.; Chaudhury, M. *Inorg. Chem.* **2012**, *51*, 7454.

(12) Perrin, D. D.; Armarego, W. L. F.; Perrin, D. R. *Purification of Laboratory Chemicals*, 2nd ed.; Pergamon: Oxford, U.K., 1980.

(13) Ali, M. A.; Livingstone, S. C.; Philips, D. J. *Inorg. Chim. Acta* **1973**, *7*, 179.

(14) Pfeiffer, P.; Breith, E.; Lülle, E.; Tsumaki, T. *Justus Liebigs Ann. Chem.* **1933**, *503*, 84.

(15) Kumar, S. B.; Bhattacharya, S.; Dutta, S. K.; Tiekink, E. R. T.; Chaudhury, M. *J. Chem. Soc., Dalton Trans.* **1995**, 2619.

(16) (a) Przychodzen, P.; Lewiński, K.; Bałanda, M.; Pełka, R.; Rams, M.; Wasiutyński, T.; Guyard-Duhayon, C.; Sieklucka, B. *Inorg. Chem.* **2004**, *43*, 2967. (b) Gerloch, M.; Lewis, J.; Mabbs, F. E.; Richards, A. *Nature* **1966**, *212*, 809.

(17) Brauer, G. *Handbook of Preparative Inorganic Chemistry*, 2nd ed.; Academic Press: New York, 1965; Vol. *2*, p 1469.

(18) Chatterjee, P. B.; Mandal, D.; Audhya, A.; Choi, K.-Y.; Endo, A.; Chaudhury, M. *Inorg. Chem.* **2008**, *47*, 3709.

(19) Gagné, R. R.; Koval, C. A.; Lisensky, G. C. *Inorg. Chem.* **1980**, *19*, 3854.

(20) Sheldrick, G. M. *SADABS, Program for Empirical Absorption Correction of Area Detector Data*; University of Göttingen: Göttingen, Germany, 1996.

(21) Sheldrick, G. M. *Acta Crystallogr.* **1990**, *46A*, 467.

(22) Sheldrick, G. M. *SHELXL-97, Program for Crystal Structure Refinements*; University of Göttingen: Göttingen, Germany, 1996.

(23) *SAINT-plus, Software users' guide*, version 6.0; Bruker Analytical X-ray Systems: Madison, WI, 1999.

(24) *DIAMOND, Visual Crystal Structure Information System*, version 3.1; Crystal Impact: Bonn, Germany, 2004.

(25) (a) Dutta, S. K.; Samanta, S.; Mukhopadhyay, S.; Burckel, P.; Pinkerton, A. A.; Chaudhury, M. *Inorg. Chem.* **2002**, *41*, 2946. (b) Samanta, S.; Ghosh, D.; Mukhopadhyay, S.; Endo, A.; Weakley, T. J. R.; Chaudhury, M. *Inorg. Chem.* **2003**, *42*, 1508. (c) Samanta, S.; Mukhopadhyay, S.; Mandal, D.; Butcher, R. J.; Chaudhury, M. *Inorg. Chem.* **2003**, *42*, 6284.
(26) Fairhurst, S. A.; Hughes, D. L.; Leigh, G. J.; Sanders, J. R.; Weisner, J. *J. Chem. Soc., Dalton Trans.* **1994**, 2591.
(27) Mathew, M.; Carty, A. J.; Palenik, G. J. *J. Am. Chem. Soc.* **1970**, *92*, 3197.
(28) Addison, A. W.; Rao, T. N.; Reedijk, J.; van Rijn, J.; Verschoor, G. C. *J. Chem. Soc., Dalton Trans.* **1984**, 1349.
(29) See for example: (a) Mandal, D.; Chatterjee, P. B.; Bhattacharya, S.; Choi, K.-Y.; Clérac, R.; Chaudhury, M. *Inorg. Chem.* **2009**, *48*, 1826. (b) Mikata, Y.; Wakamatsu, M.; So, H.; Abe, Y.; Mikuriya, M.; Fukui, K.; Yano, S. *Inorg. Chem.* **2005**, *44*, 7268. (c) Ainscough, E. C.; Brodie, A. M.; Plowman, J. E.; Browm, K. L.; Addison, A. W.; Gainsford, A. R. *Inorg. Chem.* **1980**, *19*, 3655.
(30) Goodson, P. A.; Oki, A. R.; Glerup, J.; Hodgson, D. J. *J. Am. Chem. Soc.* **1990**, *112*, 6248.
(31) Isse, A. A.; Gennaro, A.; Vianello, E. *Electrochim. Acta* **1997**, *42*, 2065.
(32) Ison, E. A.; Cessarich, J. E.; Du, G.; Fanwick, P. E.; Abu-Omar, M. M. *Inorg. Chem.* **2006**, *45*, 2385.
(33) Machura, B. *Coord. Chem. Rev.* **2005**, *249*, 591.